Supporting Information

Substituent Effects on Ni–S Bond Dissociation Energies and Kinetic Stability of Nickel Arylthiolate Complexes Supported by a Bis(phosphinite)-Based Pincer Ligand

Jie Zhang, Anubendu Adhikary, Krista M. King, Jeanette A. Krause and Hairong Guan*

Department of Chemistry, University of Cincinnati, P. O. Box 21072, Cincinnati, Ohio 45221-0172, United States

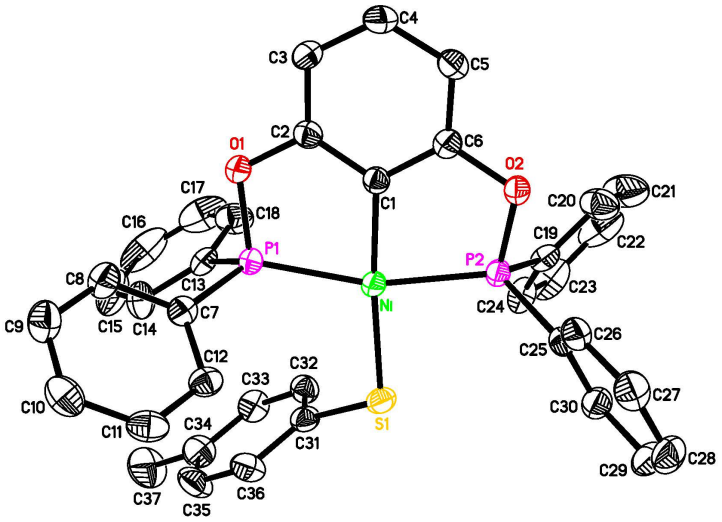

Fig. S1 ORTEP drawing of $[2,6\text{-}(Ph_2PO)_2C_6H_3]NiSC_6H_4CH_3$ (**1b**) at the 50% probability level. Hydrogen atoms are omitted for clarity.

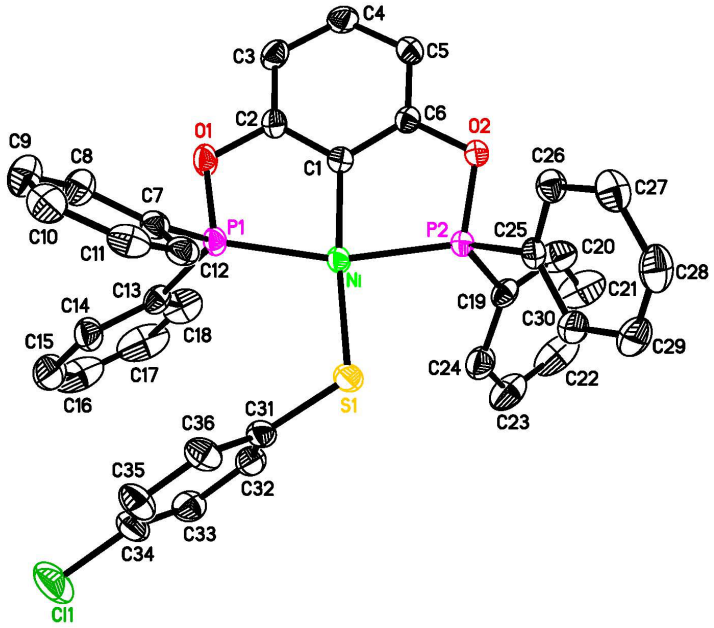

Fig. S2 ORTEP drawing of $[2,6\text{-}(Ph_2PO)_2C_6H_3]NiSC_6H_4Cl$ (**1d**) at the 50% probability level. Hydrogen atoms are omitted for clarity.

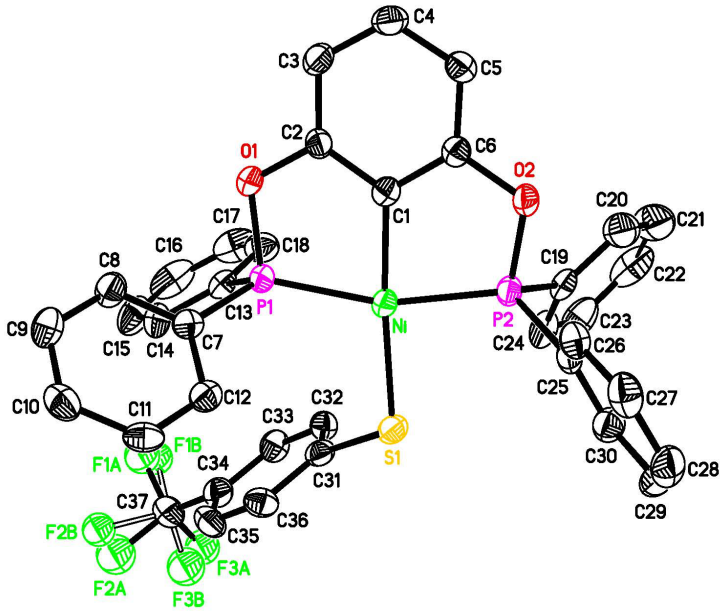

Fig. S3 ORTEP drawing of $[2,6\text{-}(Ph_2PO)_2C_6H_3]NiSC_6H_4CF_3$ (**1e**) at the 50% probability level. Hydrogen atoms are omitted for clarity. The F-atoms of the CF_3 group are disordered; a two-component model is given (70 : 30 occupancy).

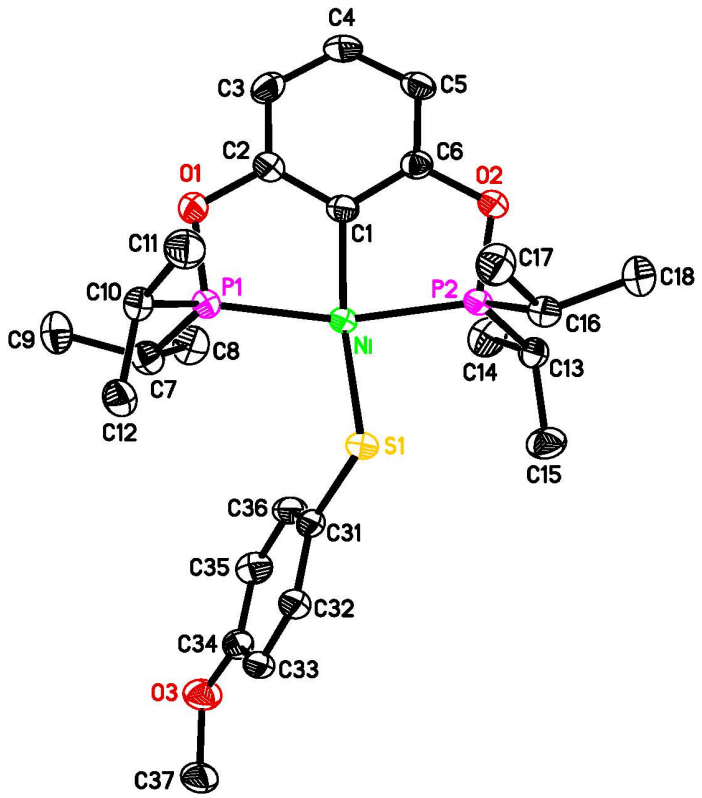

Fig. S4 ORTEP drawing of $\{2,6\text{-}[(i\text{-Pr})_2PO]_2C_6H_3\}NiSC_6H_4OCH_3$ (**2a**) at the 50% probability level. Hydrogen atoms are omitted for clarity.

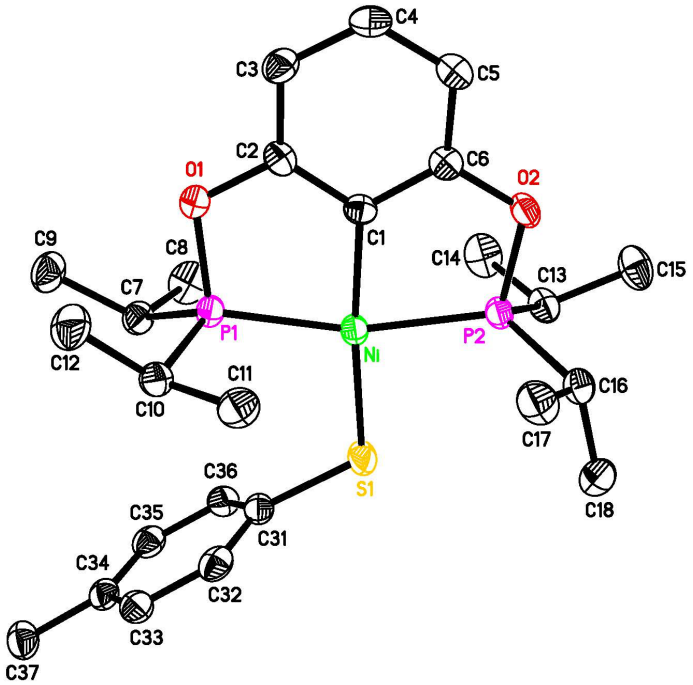

Fig. S5 ORTEP drawing of $\{2,6\text{-}[(i\text{-Pr})_2PO]_2C_6H_3\}NiSC_6H_4CH_3$ (**2b**) at the 50% probability level. Hydrogen atoms are omitted for clarity.

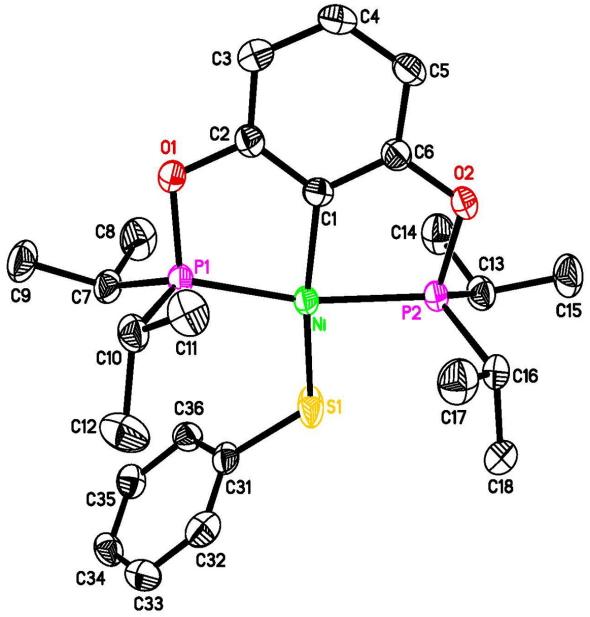

Fig. S6 ORTEP drawing of $\{2,6\text{-}[(i\text{-Pr})_2PO]_2C_6H_3\}NiSPh$ (**2c**) at the 50% probability level. Hydrogen atoms are omitted for clarity.

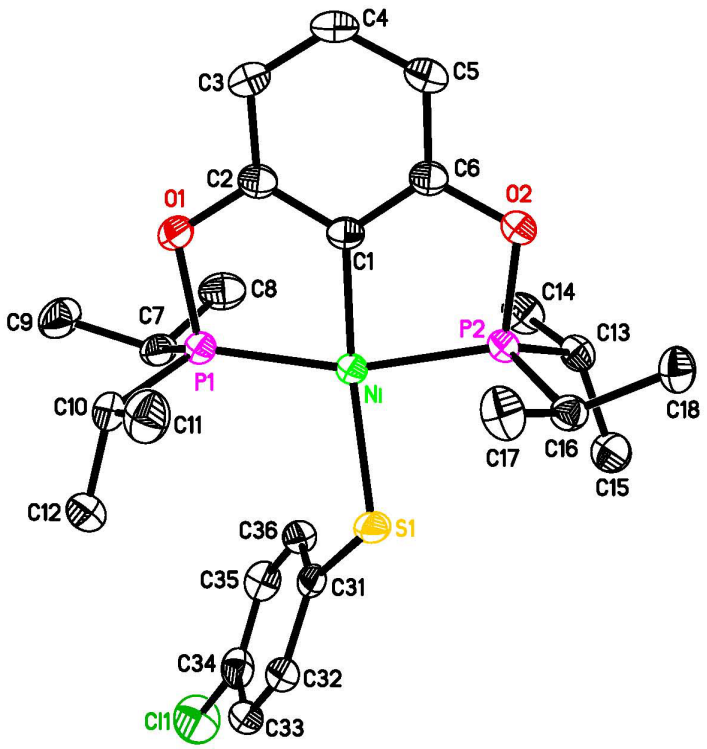

Fig. S7 ORTEP drawing of $\{2,6\text{-}[(i\text{-Pr})_2PO]_2C_6H_3\}NiSC_6H_4Cl$ (**2d**) at the 50% probability level. Hydrogen atoms are omitted for clarity.

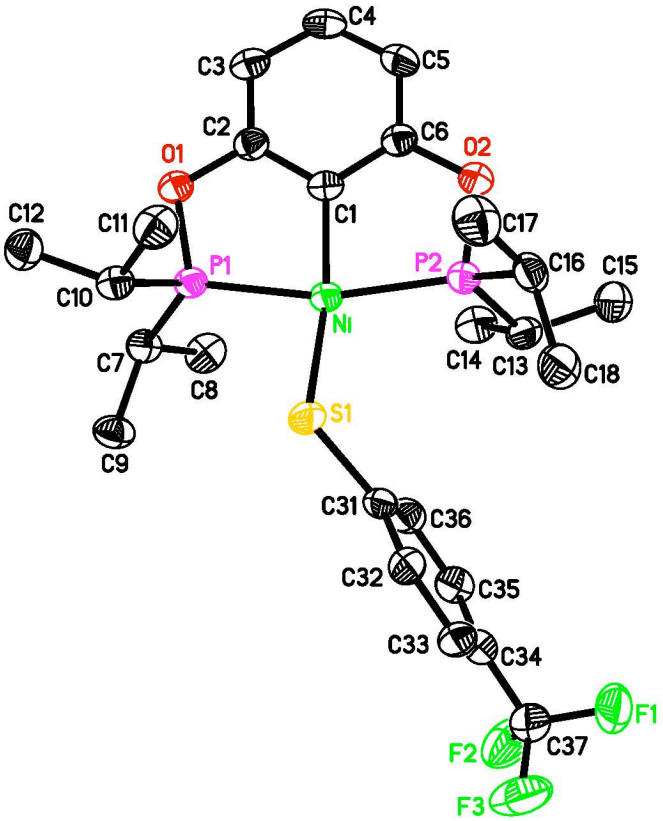

Fig. S8 ORTEP drawing of $\{2,6\text{-}[(i\text{-Pr})_2PO]_2C_6H_3\}NiSC_6H_4CF_3$ (**2e**) at the 50% probability level. Hydrogen atoms are omitted for clarity.

Table S1 Summary of crystallographic data

	1b	**1d**	**1e**	**2a**	**2b**	**2c**	**2d**	**2e**
empirical formula	$C_{37}H_{30}O_2P_2SNi$	$C_{36}H_{27}ClO_2P_2SNi$	$C_{37}H_{27}F_3O_2P_2SNi$	$C_{25}H_{38}O_3P_2SNi$	$C_{25}H_{38}O_2P_2SNi$	$C_{24}H_{36}O_2P_2SNi$	$C_{24}H_{35}O_2P_2SClNi$	$C_{25}H_{35}F_3O_2P_2SNi$
formula weight	659.32	679.74	713.30	539.26	523.26	509.24	543.68	577.24
temp, K	150(2)	150(2)	150(2)	150(2)	150(2)	150(2)	150(2)	150(2)
crystal system	monoclinic	monoclinic	monoclinic	monoclinic	triclinic	monoclinic	triclinic	triclinic
space group	$P2_1/n$	$P2_1/n$	$P2_1/n$	C2/c	P-1	$P2_1/c$	P-1	P-1
a, Å	14.8305(4)	14.7575(3)	15.0497(4)	36.0524(10)	10.2691(2)	7.8432(1)	8.5017(2)	8.6345(1)
b, Å	9.1267(2)	9.1218(2)	9.1562(2)	7.6168(2)	11.3934(2)	31.3580(5)	9.6113(2)	9.6238(2)
c, Å	24.2462(6)	24.1885(5)	24.2103(6)	25.0220(8)	13.1019(2)	10.3910(2)	16.6023(4)	16.8946(3)
α, deg	90	90	90	90	88.437(1)	90	85.405(1)	84.721(1)
β, deg	105.642(1)	105.398(1)	104.941(1)	129.255(3)	67.681(1)	94.459(1)	78.043(1)	79.927(1)
γ, deg	90	90	90	90	66.738(1)	90	88.327(1)	88.646(1)
Volume, $Å^3$	3160.27(13)	3139.25(11)	3223.34(14)	5320.6(3)	1289.15(4)	2547.90(7)	1322.80(5)	1376.34(4)
Z	4	4	4	8	2	4	2	2
d_{calc}, g/cm^3	1.386	1.438	1.470	1.346	1.348	1.328	1.365	1.393
λ, Å	1.54178	1.54178	1.54178	1.54178	1.54178	1.54178	1.54178	1.54178
μ, mm^{-1}	2.714	3.516	2.846	3.109	3.160	3.184	4.009	3.177
no. of data collected	26302	26034	26573	21489	11035	21765	11430	11813
no. of unique data	5650	5630	5601	4603	4444	4588	4586	4754
R_{int}	0.0622	0.0335	0.0731	0.0356	0.0288	0.0347	0.0225	0.0298
Goodness-of-fit on F^2	1.024	1.043	1.024	1.033	1.032	1.033	1.050	1.019
R1, wR2 ($I > 2\sigma(I)$)	0.0390, 0.0987	0.0322, 0.0851	0.0493, 0.1165	0.0321, 0.0838	0.0377, 0.0957	0.0344, 0.0867	0.0341, 0.0878	0.0407, 0.1020
R1, wR2 (all data)	0.0519, 0.1069	0.0374, 0.0888	0.0746, 0.1306	0.0379, 0.0876	0.0477, 0.1019	0.0414, 0.0916	0.0402, 0.0922	0.0526, 0.1092

Table S2 Selected bond lengths (Å) and angles (deg)

	1b	**1d**	**1e**	**2a**	**2b**	**2c**	**2d**	**2e**
Ni–S1	2.1947(7)	2.1961(5)	2.2030(10)	2.2191(6)	2.1908(7)	2.1734(6)	2.2083(6)	2.2075(8)
Ni–C1	1.907(2)	1.9088(17)	1.910(3)	1.8988(19)	1.907(2)	1.8987(19)	1.900(2)	1.899(3)
Ni–P1	2.1555(7)	2.1569(5)	2.1595(10)	2.1769(6)	2.1566(7)	2.1507(6)	2.1736(6)	2.1476(8)
Ni–P2	2.1452(7)	2.1472(5)	2.1504(10)	2.1377(6)	2.1538(7)	2.1625(6)	2.1472(6)	2.1740(8)
S1–C31	1.784(3)	1.7800(19)	1.781(4)	1.766(2)	1.789(3)	1.775(2)	1.767(2)	1.768(3)
P1–O1	1.6592(17)	1.6593(13)	1.661(2)	1.6612(14)	1.6572(17)	1.6627(14)	1.6614(15)	1.6568(18)
P2–O2	1.6446(16)	1.6470(13)	1.641(2)	1.6592(13)	1.6599(17)	1.6571(14)	1.6572(14)	1.6590(19)
O1–C2	1.390(3)	1.388(2)	1.386(4)	1.391(2)	1.391(3)	1.390(2)	1.387(3)	1.391(3)
O2–C6	1.399(3)	1.399(2)	1.403(4)	1.396(2)	1.388(3)	1.388(2)	1.390(3)	1.392(3)
P1–Ni–P2	163.10(3)	162.88(2)	162.95(4)	164.38(2)	163.27(3)	161.58(2)	163.83(3)	163.88(3)
P1–Ni–S1	103.11(3)	103.31(2)	103.03(4)	105.52(2)	104.37(3)	107.50(2)	105.03(2)	91.03(3)
P2–Ni–S1	93.79(3)	93.77(2)	94.02(4)	89.95(2)	92.24(3)	90.02(2)	91.11(2)	105.05(3)
C1–Ni–P1	81.93(7)	81.71(6)	81.77(11)	81.98(6)	81.45(7)	81.50(6)	82.06(7)	81.88(8)
C1–Ni–P2	81.17(7)	81.17(6)	81.19(11)	82.40(6)	82.00(7)	82.03(6)	81.92(7)	82.14(8)
C1–Ni–S1	174.45(7)	174.65(6)	175.00(11)	168.19(6)	173.99(8)	167.87(6)	166.69(7)	166.31(8)
C31–S1–Ni	110.85(8)	111.21(6)	110.95(12)	111.85(7)	114.07(8)	119.93(7)	114.95(7)	115.81(9)

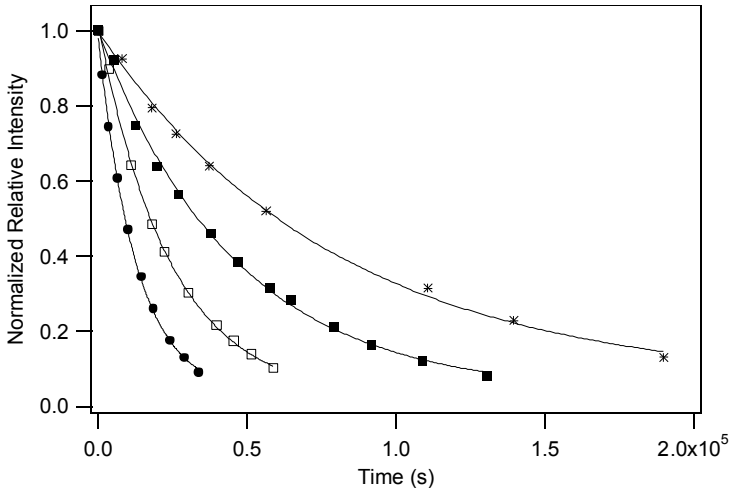

Fig. S9 Sample plots of two-parameter fit in KaleidaGraph: k_{obs} for the reaction between [2,6-$(Ph_2PO)_2C_6H_3$]NiSPh (**1c**) and benzyl bromide ([**1c**]$_0$ = 0.018 M, [$PhCH_2Br$]$_0$ = 0.18 M) in toluene-d_8 at various temperatures (∗: 50°C; ■ : 60°C; □: 70°C; ● : 80°C).

Table S3 k_{obs} for the reaction between [2,6-$(Ph_2PO)_2C_6H_3$]NiSPh (**1c**) and benzyl bromide in toluene-d_8 at various temperatures.

Temperature	[**1c**]$_0$ (M)	[$PhCH_2Br$]$_0$ (M)	k_{obs} (s^{-1})
50 °C	0.018	0.18	$1.3(1) \times 10^{-5}$
50 °C	0.018	0.23	$1.7(1) \times 10^{-5}$
50 °C	0.018	0.28	$2.0(1) \times 10^{-5}$
50 °C	0.018	0.33	$2.4(1) \times 10^{-5}$
60 °C	0.018	0.18	$2.2(1) \times 10^{-5}$
60 °C	0.018	0.23	$3.0(1) \times 10^{-5}$
60 °C	0.018	0.28	$3.8(1) \times 10^{-5}$
60 °C	0.018	0.33	$4.3(1) \times 10^{-5}$
70 °C	0.018	0.18	$4.0(2) \times 10^{-5}$
70 °C	0.018	0.23	$5.5(1) \times 10^{-5}$
70 °C	0.018	0.28	$7.0(3) \times 10^{-5}$
70 °C	0.018	0.33	$8.5(2) \times 10^{-5}$
80°C	0.018	0.18	$8.3(4) \times 10^{-5}$
80°C	0.018	0.23	$1.1(1) \times 10^{-4}$
80°C	0.018	0.30	$1.5(1) \times 10^{-4}$
80°C	0.018	0.33	$1.7(1) \times 10^{-4}$

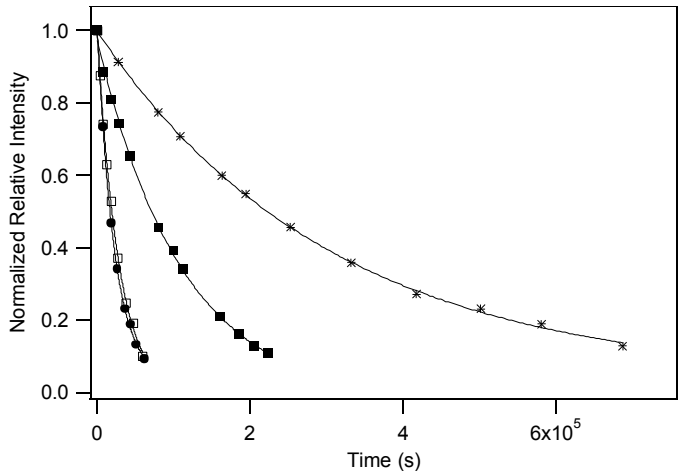

Fig. S10 Sample plots of two-parameter fit in KaleidaGraph: k_{obs} for the reaction between [2,6-$(Ph_2PO)_2C_6H_3$]$NiSC_6H_4Z$ (**1a**, **1b**, **1d**, **1e**) and benzyl bromide ([**1**]$_0$ = 0.020 M, [$PhCH_2Br$]$_0$ = 0.20 M) in toluene-d_8 at 60 °C (∗: **1e**; ■: **1d**; □: **1b**; ●: **1a**).

Table S4 k_{obs} for the reactions between [2,6-$(Ph_2PO)_2C_6H_3$]$NiSC_6H_4R$ (**1a**, **1b**, **1d**, **1e**) and benzyl bromide in toluene-d_8 at 60°C.

complex	[Ni]$_0$ (M)	[$PhCH_2Br$]$_0$ (M)	k_{obs} (s^{-1})
1a	0.015	0.15	$4.4(1) \times 10^{-5}$
1a	0.015	0.20	$5.4(1) \times 10^{-5}$
1a	0.015	0.25	$6.3(4) \times 10^{-5}$
1a	0.015	0.33	$8.9(2) \times 10^{-5}$
1b	0.020	0.20	$3.7(2) \times 10^{-5}$
1b	0.019	0.25	$4.1(1) \times 10^{-5}$
1b	0.015	0.30	$5.4(3) \times 10^{-5}$
1b	0.015	0.35	$5.9(1) \times 10^{-5}$
1d	0.020	0.20	$1.0(1) \times 10^{-5}$
1d	0.020	0.25	$1.2(1) \times 10^{-5}$
1d	0.020	0.30	$1.4(1) \times 10^{-5}$
1d	0.020	0.35	$1.7(1) \times 10^{-5}$
1e	0.020	0.20	$3.3(1) \times 10^{-6}$
1e	0.020	0.25	$4.0(1) \times 10^{-6}$
1e	0.020	0.30	$4.8(1) \times 10^{-6}$
1e	0.020	0.35	$5.9(1) \times 10^{-6}$

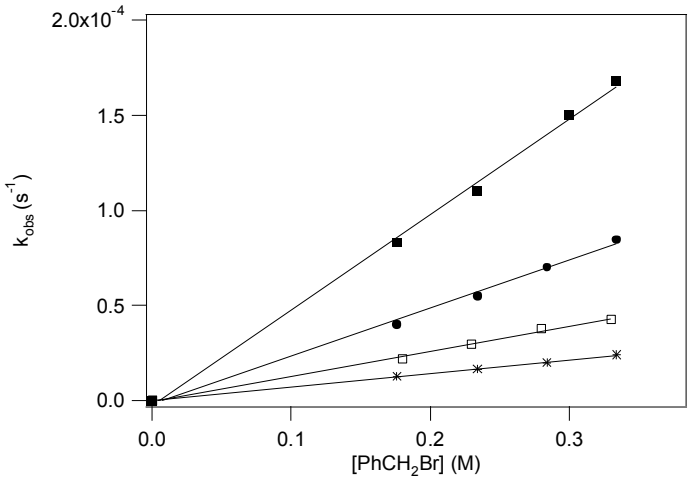

Fig. S11 Plots of k_{obs} versus concentration of benzyl bromide for the reaction of [2,6-$(Ph_2PO)_2C_6H_3$]NiSPh (**1c**) with benzyl bromide in toluene-d_8 at various temperatures (■: 80°C; ●: 70°C; □: 60°C; ∗: 50°C)

Table S5 Summary of the second-order rate constants k for the reaction of [2,6-$(Ph_2PO)_2C_6H_3$]NiSPh (**1c**) with benzyl bromide in toluene-d_8 at various temperatures.

T (K)	1/T (K^{-1})	k ($s^{-1}M^{-1}$)	ln(k/T)
323	0.00310	$7.1(3) \times 10^{-5}$	-15.33
333	0.00300	$1.4(1) \times 10^{-4}$	-14.68
343	0.00292	$2.8(1) \times 10^{-4}$	-14.02
353	0.00283	$5.4(2) \times 10^{-4}$	-13.39

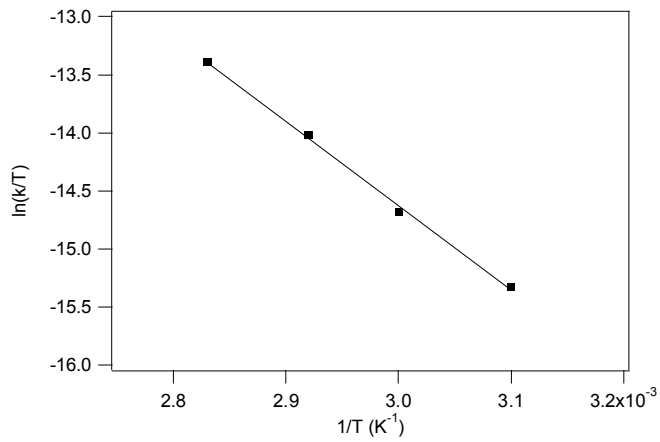

Fig. S12 An Eyring plot for the reaction of [2,6-$(Ph_2PO)_2C_6H_3$]NiSPh (**1c**) with benzyl bromide in toluene-d_8 between 50 °C and 80 °C.

$$\Rightarrow \quad \Delta H^{\ddagger} = 61.5 \pm 0.8 \text{ kJ mol}^{-1} \text{ and } \Delta S^{\ddagger} = -135.1 \pm 2.9 \text{ J K}^{-1} \text{ mol}^{-1}$$

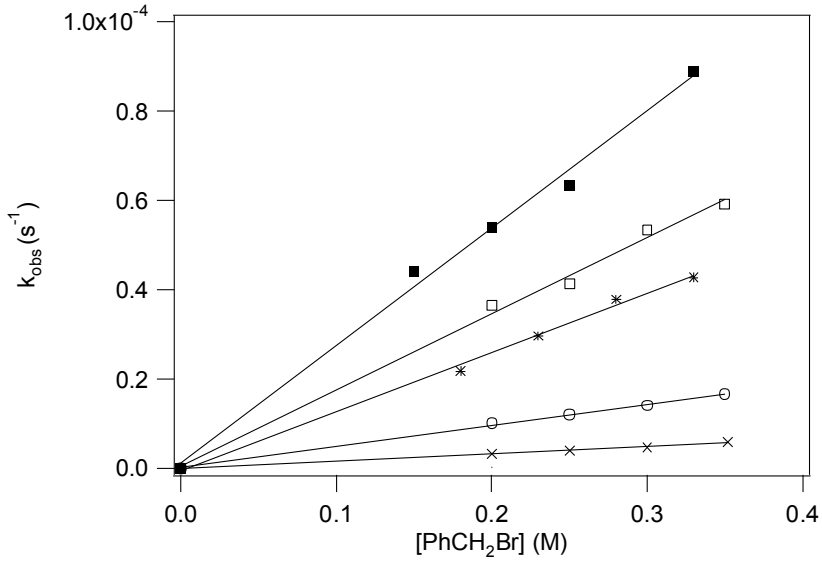

Fig. S13 Plots of k_{obs} versus concentration of benzyl bromide for the reaction of [2,6-$(Ph_2PO)_2C_6H_3$]$NiSC_6H_4Z$ (**1a-e**) with benzyl bromide in toluene-d_8 at 60 °C (■: **1a**; □: **1b**; ∗: **1c**; ○: **1d**; ×: **1e**).

Table S6 Summary of second-order rate constants *k* for the reactions of $[2,6\text{-}(Ph_2PO)_2C_6H_3]NiSC_6H_4Z$ (**1a-e**) with benzyl bromide in toluene-d_8 at 60 °C.

Complex	**1a**	**1b**	**1c**	**1d**	**1e**
k ($s^{-1}M^{-1}$)	$2.5(2) \times 10^{-4}$	$1.6(2) \times 10^{-4}$	$1.4(1) \times 10^{-4}$	$4.4(2) \times 10^{-5}$	$1.7(1) \times 10^{-5}$

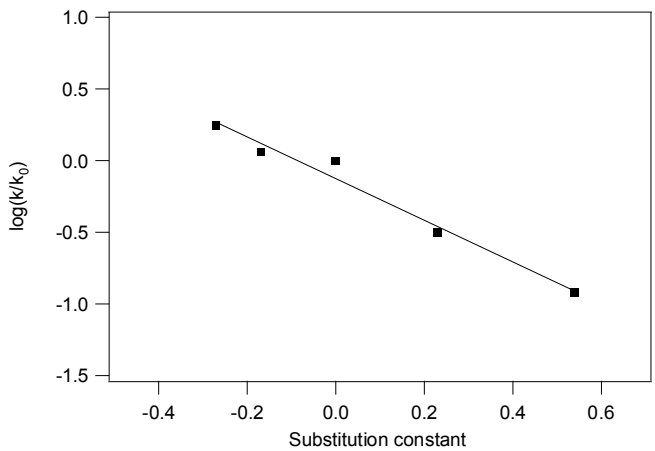

Fig. S14 Hammett plot for the second-order rate constants *k* of the reaction of $[2,6\text{-}(Ph_2PO)_2C_6H_3]NiSC_6H_4Z$ (**1a-e**) with benzyl bromide at in toluene-d_8 60 °C.

$$\Rightarrow \rho = -1.5 \pm 0.3$$

Table S7 k_{obs} for the reactions between $\{2,6\text{-}[(i\text{-}Pr)_2PO]_2C_6H_3\}NiSC_6H_4Z$ (**2a** and **2c**) and benzyl bromide in toluene-d_8 at 60°C.

complex	$[Ni]_0$ (M)	$[PhCH_2Br]_0$ (M)	k_{obs} (s^{-1})
2a	0.014	0.14	$6.0(4) \times 10^{-5}$
2a	0.014	0.18	$8.1(2) \times 10^{-5}$
2a	0.014	0.21	$9.9(4) \times 10^{-5}$
2a	0.014	0.25	$1.1(1) \times 10^{-4}$
2c	0.014	0.14	$2.5(2) \times 10^{-5}$
2c	0.014	0.18	$3.1(4) \times 10^{-5}$
2c	0.014	0.21	$3.6(2) \times 10^{-5}$
2c	0.014	0.25	$4.4(2) \times 10^{-5}$

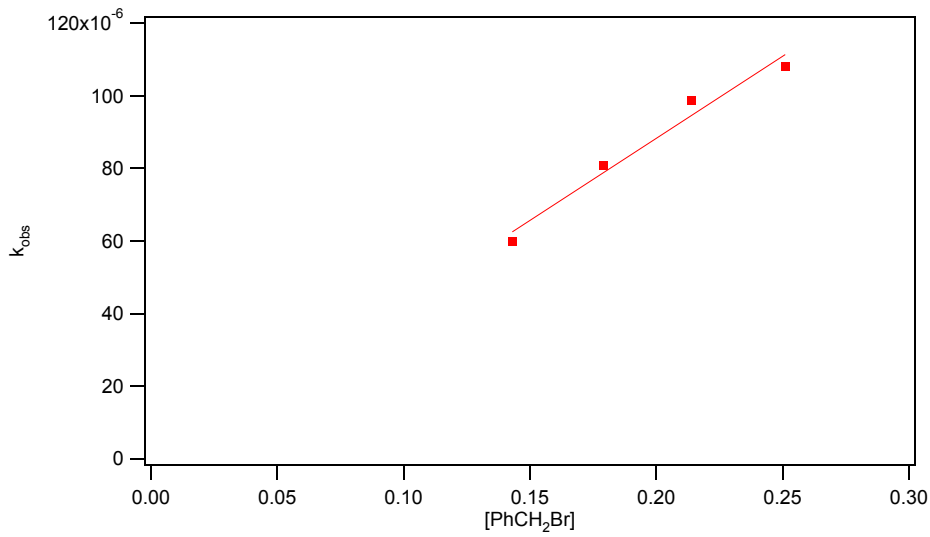

Fig. S15 Plot of k_{obs} versus concentration of benzyl bromide for the reaction of {2,6-[(*i*-Pr)$_2$PO]$_2$C$_6$H$_3$}NiSC$_6$H$_4$OCH$_3$ (**2a**) with benzyl bromide in toluene-d_8 at 60 °C.

$$k = 4.5(5) \times 10^{-4}\ \mathrm{M^{-1}s^{-1}}$$

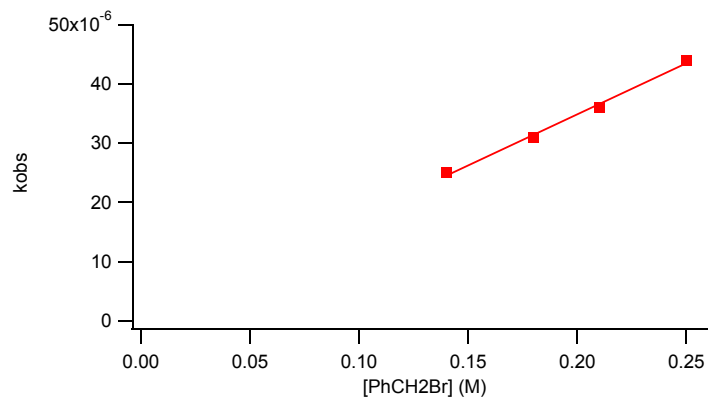

Fig. S16 Plot of k_{obs} versus concentration of benzyl bromide for the reaction of {2,6-[(*i*-Pr)$_2$PO]$_2$C$_6$H$_3$}NiSC$_6$H$_5$ (**2c**) with benzyl bromide in toluene-d_8 at 60 °C.

$$k = 1.7(1) \times 10^{-4}\ \mathrm{M^{-1}s^{-1}}$$